

# Design and Performance Evaluation of an Air-Blast Atomizer

Dr. Olusegun Adefonabi Adefuye  
Department of Mechanical Engineering,  
Lagos State University,  
Lagos, Nigeria

Benneth Ifenna Okoli  
Centre for Space Transport and Propulsion,  
National Space Research and Development Agency,  
Abuja, Nigeria

---

**Abstract:** The present work describes the design, construction and experimental investigations of an air-blast atomizer for half spray cone angle of 30° using stainless steel for foundry application. Outline detail of experimental setup to investigate effect of injection pressures on spray and flame lengths, the amount of fuel and the time taken to melt some selected materials was studied. An experimental study of air-blast atomization was conducted using the manufactured atomizer in which the fuel (kerosene) flows under gravity at angle 45° from the tank and was atomized by the oxygen stream flowing in a cylindrical channel from a pressurized oxygen bottle (cylinder). Produced air-blast atomizer was experimentally investigated at different pressures ranging from 3 to 15 bars in the step of 3 bars [6].

As the injection pressure was increased from 3 to 15 bars, the spray and flame lengths increases. From 6 to 12 bars, visible increment was observed in the spray and flame lengths due to increase in injected pressure which led to breaking-up of the liquid film into small droplets. As enough pressure was provided from 12 to 15 bars, spray and flame lengths increased appreciably. 0.6 kg of aluminum melted in 13 minutes 43 seconds using 0.5 liter of kerosene; the volumetric flow rate and the mass flow rate obtained was  $6.075 \times 10^{-7} \text{ m}^3/\text{sec}$  and  $4.921 \times 10^{-4} \text{ kg}/\text{sec}$  respectively. Similarly, 1.2 kg of brass melted in 17 minutes 13 seconds using 1 liter of kerosene; the volumetric flow rate and the mass flow rate obtained was  $9.680 \times 10^{-7} \text{ m}^3/\text{sec}$  and  $7.841 \times 10^{-4} \text{ kg}/\text{sec}$  respectively. The furnace efficiency of 2.2 % was calculated from the theoretical and actual energy used for melting the metal [6].

**Keywords:** Air-blast atomizer; stainless steel; kerosene; spray cone angle; furnace; foundry.

---

## 1. INTRODUCTION

Atomization is a process whereby a volume of liquid is converted into a multiplicity of small drops [1]. Its principal aim is to produce a high ratio of surface to mass in the liquid phase, resulting in very high evaporation rates. Air-blast atomizers have many advantages over pressure atomizers, especially in their application to gas turbine engines of high pressure ratio. They require lower fuel pressures and produce a finer spray. Moreover, because the air-blast atomization process ensures thorough mixing of air and fuel, the ensuing combustion process is characterized by very low soot formation and a blue flame of low luminosity, resulting in relatively cool liner walls and a low exhaust smoke. The merits of the air-blast atomizer have led in recent years to its installation in a wide range of industrial and aircraft engines. Most of the systems now in service are of the “pre-filming” type, in which the fuel is first spread out into a thin, continuous sheet and then subjected to the atomizing action of high velocity air. In other designs, the fuel is injected into the high-velocity airstream in the form of one or more discrete jets. In all cases the basic objective is the same, namely, to deploy the available air in the most effective manner to achieve the best possible level of atomization [1].

Madu [2] designed, constructed and tested a burner that uses an admixture of used engine oil and kerosene for foundry application. Tests were carried out to determine the time taken to melt 1 kg each of the selected engineering materials (copper, aluminum, brass, and lead). It took 49 minutes, 15

minutes, 22 minutes, and 7 minutes to melt copper, aluminum, brass, and lead respectively.

Robert [3] studied the effect of atomization gas properties on droplet atomization in an air-assist atomizer where air and fuel mix within the nozzle before exiting through the outlet orifice. He used air, nitrogen, argon, and carbon dioxide as the atomizing gas to determine the effect of each of these gases on mean droplet size, number density, velocity and their distributions in kerosene fuel sprays. Data were obtained with these atomizing gases using a base, air assisted case as a reference. Comparisons were made between the gases on a mass and momentum flux basis. The results show that the presence of oxygen in the air atomized sprays assists in the combustion process, since it produces smaller and faster moving droplets, especially at locations near to the nozzle exit. Lighter gases such as nitrogen more effectively atomized the fuel in comparison to the denser gases. Argon and carbon dioxide produced larger, slower moving droplets than air and nitrogen assisted cases.

Witold [10] studied kerosene atomization process under high speed air stream. Experiments showed that in the case of stream-type injectors (atomizers), a large number of small injection holes in detonation chamber should be applied in relation to disintegration of injected fuel as well as spatial uniformity of created combustible mixture.

Pipatpong [11] developed an air-assisted fuel atomizer for a continuous combustor. They summarized that low pressure air atomization of refined palm oil fuel with air pressure in the range of 69 – 620 kPa can be used to develop air blaster or burners.

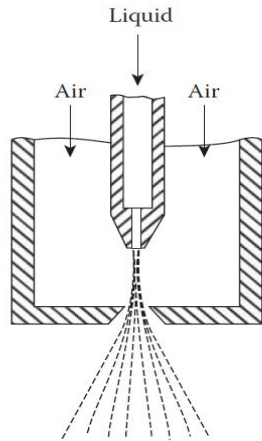


Figure 1: Schematic of an air-blast atomizer [4].

## 2. MATERIALS AND METHODOLOGY

### 2.1 Materials selection

The selection of materials to be used for the different components in this design involves the following consideration:

- i. Cost and availability of the material.
- ii. Material property – mechanical, physical and chemical properties (that is, its ability to resist corrosion due to prolonged usage).

### 2.2 Properties of fuel used

The kerosene fuel sample was collected from Nigerian National Petroleum Corporation (NNPC) approved gas station in Lagos – Nigeria. The specification of the fuel is presented below.

Table 1: Properties of fuel used [5].

Property	Unit	Kerosene
Chemical formula	-	C <sub>10</sub> H <sub>22</sub>
Calorific value	kJ/kg	45400
Self-ignition temperature	°C	640
Final boiling point	°C	249
Ignition delay period	S	0.0015
Flame propagation rate	cm/s	11.8
Flame temperature	°C	1782
Kinematic viscosity @ 39°C	m <sup>2</sup> /s	2.2
Specific gravity @ 15.6/15.6 °C	-	0.843
Colour	-	Colourless
Sulphur content	wt %	0.04

Table 2: Other materials used and their properties

S/N	Parts	Material Selected	Material Property
1	Fuel tank	Mild steel	Strength and ability to resist corrosion.
2	Hose	i. Galvanized	i. Ability to resist corrosion.

		ii. Polymer	ii. Chemically inert to oil.
3	Fuel stand	Mild steel	Strength and ability to resist corrosion.

### 2.3 Design considerations for the atomizer

The air passage should be made aerodynamically smooth, with minimum areas at the atomization edge to obtain maximum air velocities and to maintain them during initial disintegration process. The cylindrical part of the injector nozzle should be short; an increase of nozzle length is undesirable, since it leads to a decrease of the root angle of the spray. It is recommended that the cone angle on the horizontal entrance be within limits from 60° to 120° [7]. It is advisable to calculate these parameters on the basis of the theory of the spray, using the curves shown below:

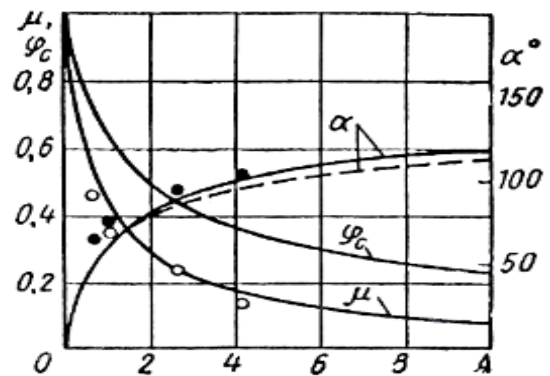


Figure 2: Dependence of discharge coefficient  $\mu$ , nozzle space factor  $\phi$  and spray angle  $\alpha$  on the geometric characteristic of the injector A - experimental points [7].

Determining the dimension of the air-blast atomizer from Figure 2; the spray angle  $\alpha$  was chosen to be 60°. Diameter of the nozzle orifice,  $d_c$  was calculated using equations 1 and 2 below:

$$d_c = \sqrt{\frac{4G}{\pi C_d \sqrt{2\rho\Delta P}}} \quad (1)$$

Where:

G = mass flow rate

$C_d = 0.27$  = discharge coefficient (from Figure 2)

$\rho = 810 \text{ kg/m}^3$  = density of kerosene

$P_1 = 3 \text{ bars} = 300,000 \text{ Pa}$  = injected pressure

$P_{\text{atm.}} = 101,300 \text{ Pa}$  = atmospheric pressure

$\Delta P = P_1 - P_{\text{atm.}} = 198,700 \text{ Pa}$  = pressure differential

But,

$$G = \rho Q = C_d A \sqrt{2\rho\Delta P} \quad (2)$$

The effect of viscosity on the atomizer (nozzle) is given by the Reynolds number at the inlet of the atomizer:

$$Re = \frac{4G}{\pi \rho g \sqrt{id_c}} \quad (3)$$

Where:

$C_d$  the contraction coefficient (assumed from the range of 0.85 - 0.90) [9].  $d_c$  is the diameter of the nozzle. After calculation of  $d_c$ , other geometrical sizes of the injector: the nozzle length  $l_c$ , length of entrance port  $l_{oz}$ , diameter of inlet port  $d_{oz}$ , was selected based on [8] approach.

**Table 3: Design parameters for the air-blast atomizer**

Design Data	Nozzle half spray angle 30°
Diameter of nozzle, $d_c$	0.89 mm
Number of inlet ports, n	2
Diameter of inlet port, $d_{oz}$	3 mm
Length of entrance port, $l_{oz}$	40 mm
Nozzle Length, $l_c$	50 mm

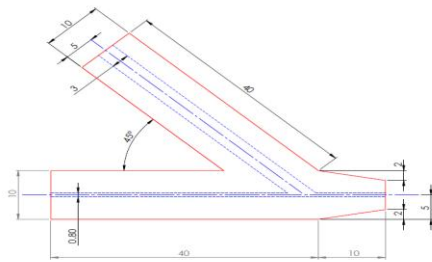


**Figure 3: Manufacturing diagram of the atomizer [6].**

## 2.4 Flow of kerosene from the fuel tank to the atomizer

Using the energy conservation concept to determine the velocity of flow along a pipe from a reservoir, we considered the ideal reservoir in Figure 4 below.

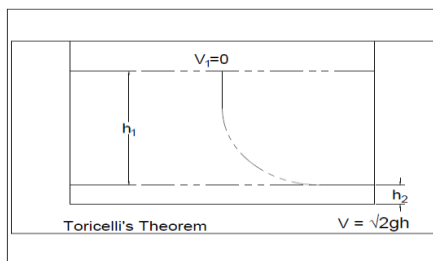


**Figure 4: An ideal reservoir.**

The level of the fuel in the reservoir is  $h_1$ . Considering the energy situation – there is no movement of the fuel, so kinetic energy is zero but the gravitational energy is:

$$mgh \quad (4)$$

If the pipe is attached at the bottom, fuel flows along this pipe out of the tank to a level  $h_2$ . A mass,  $m$  has flowed from the top of the reservoir to the nozzle and it has gained a velocity,  $v$ .

So, from Torricelli's equation:

$$v = \sqrt{2g(h_1 - h_2)} \quad (5)$$

We now have an expression for the velocity of the fuel as it flows from the fuel tank to the atomizer at a height ( $h_1 - h_2$ ) below the surface of the reservoir.

Where:

$h_1 = 2.1$  m = height of fuel tank stand + height of fuel level in the tank

$h_2 = 0$  = height of atomizer (ground level)

$g = 9.81$  m/s<sup>2</sup> = acceleration due to gravity

$\rho = 810$  kg/m<sup>3</sup> = density of kerosene

**Fuel velocity,  $v$**

$$v = \sqrt{2g(h_1 - h_2)} \quad (6)$$

$$v = \sqrt{2 * 9.81 * 2.1} = 6.42 \text{ m/s}$$

**Pressure inside the fuel pipe,  $P$**

$$P = \rho gh \quad (7)$$

$$= 810 * 9.81 * 2.1 = 16686.81 \text{ Pa}$$

## 2.5 Separation losses in pipe flow

These are losses which occur as a result of various pipes fittings such as bends, valves, and also sudden enlargement and contraction of the pipe. For losses due to friction, using Darcy -Weisbach equation:

$$h_f = f \frac{l}{d} \frac{v^2}{2g} \quad (8)$$

But, Reynolds number for a pipe is given by:

$$Re = \frac{\rho v d_h}{u} = \frac{v d_h}{u} \quad (9)$$

Where:

$v = 6.4$  m/s = fuel velocity

$u =$  kinematic viscosity (1 cst =  $10^{-6}$  m<sup>2</sup>/s) =  $2.2 * 10^{-6}$  m<sup>2</sup>/s

$d_h =$  hydraulic diameter

$$d_h = \frac{4(\pi r_o^2 - \pi r_i^2)}{(2\pi r_o + 2\pi r_i)} = 2(r_o - r_i) \quad (10)$$

$d_o = 0.0102$  m = external diameter of fuel pipe,  $r_o = 5.1 * 10^{-3}$  m = external radius of fuel pipe.

$d_i = 0.01$  m = internal diameter of fuel pipe,  $r_i = 5 * 10^{-3}$  m = internal radius of fuel pipe.

$$d_h = 2 * 10^{-4} \text{ m} \quad \text{and} \quad \text{Re} = \frac{\rho v d_h}{\mu} = \frac{v d_h}{\nu}$$

Where:

$d_i$  = 0.01 m = internal diameter of fuel pipe

$h_f$  = head loss due to friction in the pipe

$f$  = friction coefficient

$v$  = 6.42 m/s = fuel velocity

$l$  = 2.97 m = length of fuel pipe

$$\text{Re} = 583.64 \text{ Pa}$$

Since the flow is laminar as Reynolds number is less than 2000,

$$f = \frac{64}{\text{Re}} = 0.11$$

$$\therefore h_f = f \frac{l}{d} \frac{v^2}{2g} = 64.42 \text{ Pa}$$

## 2.6 Test facility

A schematic of the test facility is shown in Figure 6, the atomizer was mounted on a thick plate for support and the fuel and oxygen pipes were fixed to the adaptors. The oxygen for the test was provided from oxygen refrigerant cylinder of 150 bars pressure capacity. A pressure regulator was used to keep the pressures constant at any pressure injection feed. The different parts of the atomizer were assembled together in the following order: the oxygen inlet and fuel inlet adapter was bolted to the atomizer and finally, the fuel hose and the oxygen hose was connected to the fuel inlet and to the oxygen inlet adapter respectively. The burning device operates on the principle of combustion in which oxygen (air) is required or supplied to enhance burning [6].

## 2.7 Experimental investigations

The fuel (kerosene) was stored in a tank of 0.8 m length and 0.4 m diameter mild steel of 27 litres capacity, the liquid flows under gravity and injected through a small diameter orifice at the centerline of the atomizer. A calibrated valve was used to regulate the flow of kerosene from the fuel tank. Pressurized oxygen (air) was injected through a pipe to the fuel pipe and the fuel drops through the pipe duct at an angle of 45° to form the liquid streams. The nozzle increases the velocity of the fluid [6].

The experimental setup was developed for the measurement of spray characteristics like spray lengths and flame lengths at different pressures varying from 3 to 15 bars. Photographs were taken by high speed camera to capture the spray lengths and flame lengths at different injected pressures. Also the time taken to melt the selected materials was also obtained.

### 2.7.1 Determination of spray lengths at different injected pressures

The rate of flow of fuel from the tank was kept constant for all the experiments by controlling the valve. The pressurized oxygen and kerosene were well mixed before exiting the atomizer. Visible atomization process was observed as the mixture of oxygen and kerosene was seen discharging through the atomizer (nozzle) orifice. Using a pressure regulator attached to the oxygen bottle; at different injected pressures ranging from 3 to 15 bars, the spray lengths were captured using a camera [6].

### 2.7.2 Determination of flame lengths at different injected pressures

The pressurized oxygen and kerosene were well mixed before exiting the atomizer. Visible atomization process was observed as the mixture of oxygen and kerosene was seen discharging through the atomizer (nozzle) orifice. The atomizer sprays the mixture and it was ignited using a lighter. With the help of the pressure regulator attached to the oxygen bottle; at different injected pressures ranging from 3 to 15 bars, the flame lengths were captured using a camera [6].

### 2.7.3 Determination of time taken to melt metal charge

The volume of kerosene in the fuel tank was noted. The crucible pot and the metal charge to be melted was prepared and weighed using digital weighing machine. The crucible pot with the metal inside was placed in a pit furnace and the taps that controls the fuel and the oxygen line was opened. Once visible atomization process was observed the fuel was ignited. As the fuel was ignited, a stop watch was used to check how long it took to melt a particular metal. Before and after each test (melting of the metals), the volume of kerosene was noted and the difference between the initial and the final volume gives the amount of kerosene used to melt the metal [6].

## 3. RESULTS AND DISCUSSIONS



Figure 5: Designed atomizer [6].



Figure 6: Complete assembly of the system [6].

Table 4: Spray lengths at different injection pressures (Measured values)

S/N	Pressures (Bars)	Spray lengths (mm)
1	3	604
2	6	832
3	9	1071
4	12	1506
5	15	1785

Figures 7 to 11 shows the sprays from the produced atomizer having half spray angle of  $30^\circ$  at different injected pressures.

Figure 7 shows that entrainment of secondary air starts beyond 400 mm. As velocity of the spray decreases as it leaves the nozzle, the spreading of the spray becomes more pronounced because of the decrease in the velocity of the spray.



Figure 7: Spray for  $\alpha = 60^\circ$  and  $\Delta P = 3$  bars.

Figure 8 shows that entrainment of secondary air starts beyond 700 mm. As velocity of the spray decreases as it leaves the nozzle, the spreading of the spray becomes more pronounced because of the decrease in the velocity of the spray.



Figure 8: Spray for  $\alpha = 60^\circ$  and  $\Delta P = 6$  bars.

Figure 9 shows a jet which was produced when the fluid (oxygen and kerosene) was discharged through the nozzle. The spray was linear up to 600 mm because the velocity at the tip of the nozzle is more which extends until was affected by the air from the atmosphere. Beyond point 600 mm, entrainment of secondary air occurs. The free jet was produced when the fluids was discharged in the surrounding with no confinement.



Figure 9: Spray for  $\alpha = 60^\circ$  and  $\Delta P = 9$  bars.

The spray as observed in Figure 10 shows that entrainment of secondary air starts around 700 mm; before this point, the spray was seen to be linear because the velocity of the spray was greater at that region. The entrainment of the surrounding in the jet increases the mass of the jet but decreases the velocity of the jet as it sprays.



Figure 10: Spray for  $\alpha = 60^\circ$  and  $\Delta P = 12$  bars.

The entrainment of the surrounding as observed (beyond 900 mm) in Figure 11 was due to increase in mass of jet which depends on the difference in the momentum flux within the jet and that of the surrounding (note that as the jet was discharged into a still surrounding, the surrounding was set in motion). The entrainment of the surrounding will continue as long as the difference in the momentum flux exists.



**Figure 11: Spray for  $\alpha = 60^\circ$  and  $\Delta P = 15$  bars.**

Figures 12 to 16 shows the flames from the produced atomizer having half spray angle of  $30^\circ$  for different injected pressures.

**Table 5: Flame lengths at different pressures (Measured values)**

S/N	Pressures (Bars)	Flame lengths (mm)
1	3	903
2	6	1102
3	9	1401
4	12	1608
5	15	1804

The free unconfined jet spreads in the surrounding and the entrainment of the secondary air occurred around 400 mm as observed in Figure 12. The spreading of the flame was due to entrainment of the surrounding. The free jet has no confinement and hence can spread till the difference between the momentum flux (mass of the jet \* velocity of the jet) of the jet and the surrounding becomes zero. Entrainment of surrounding depends on mass flow rate and jet velocity.



**Figure 12: Flame for  $\alpha = 60^\circ$  and  $\Delta P = 3$  bars.**

Due to entrainment of the surrounding as observed in Figure 13, the axial velocity of the jet decreases making the flame to start spreading beyond 600 mm. Because of the increased velocity of the jet, the flame as seen in the Figure was linear without any interference from the surrounding air.



**Figure 13: Flame for  $\alpha = 60^\circ$  and  $\Delta P = 6$  bars.**

In Figure 14, the characteristic feature of the flame as it spreads was due to the difference in the density of the jet and the surrounding. A hot jet in a cold surrounding spreads faster than a cold jet in the same surrounding. Spreading of the flame which started to occur beyond 1200 mm was due to entrainment of the surrounding.



**Figure 14: Flame for  $\alpha = 60^\circ$  and  $\Delta P = 9$  bars.**

Figure 15 shows that the flame starts spreading as a result of the surrounding air beyond point 1300 mm.



**Figure 15: Flame for  $\alpha = 60^\circ$  and  $\Delta P = 12$  bars.**

Figure 16 shows that the spreading of the hot flame as a result of the surrounding air started beyond point 1500 mm. It was

observed that there was a whitish flame formed very close to the tip of the atomizer; the flame was at the region where the velocity of the jet is high without entrainment of the secondary air. The whitish flame indicates that there was complete combustion process of the fuel.



**Figure 16: Flame for  $\alpha = 60^\circ$  and  $\Delta P = 15$  bars.**

The graph in Figure 17 was gotten from the regression analysis of the two sample items, the injection pressure and the spray lengths. After the calculations, a relationship between the pressures and the spray lengths was established, thus the graph. The equation of best fitting line that described all the points was established and the straight line graph was plotted. At any point on y or x axis the other corresponding values can be obtained from the other axis. It was also proven that the two sample items (the pressure and spray length or flame length as the case may be) has a linear relationship that exists between them.

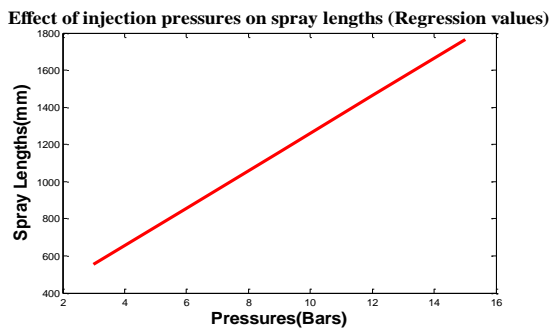


**Figure 17: Effect of injected pressures on spray lengths.**

The graph in Figure 18 was gotten from the regression analysis of the two sample items, the injection pressure and the flame lengths. After the calculations, a relationship between the pressures and the flame lengths was established, thus the graph. The equation of best fitting line that described all the points was established and the straight line graph was plotted. At any point on y or x axis the other corresponding values can be obtained from the other axis. It was also proven that the two sample items (the pressure and flame length) has a linear relationship that exists between them.

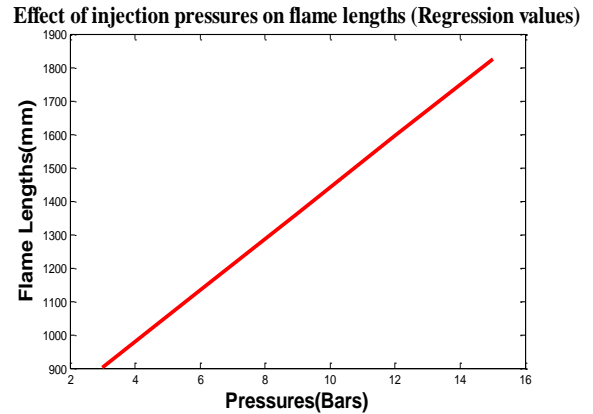


**Figure 18: Effect of injected pressures on flame lengths.**

Figure 19 is the graph of measured spray lengths versus injected pressures and regression values of spray lengths versus injected pressures plotted to compare how close the points (measured spray lengths and regression values of spray lengths) are. The graph of injection pressures versus the regression values of spray lengths is a linear graph but that is not the case of the graph for injection pressures versus the measured spray values; the discrepancies in the profile of the measured spray lengths was from errors while taking the readings.

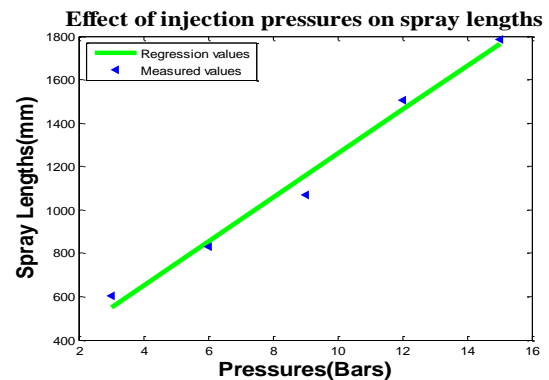


**Figure 19: Effect of injected pressures on spray lengths (measured and regression values).**

Figure 20 is the graph of measured flame lengths versus injected pressures and regression values of flame lengths versus injected pressures plotted to compare how close the points (measured flame lengths and regression values of flame lengths) are. From the graph it can be deduced that the readings gotten for the measured flame lengths and the corresponding regression values of flame lengths are almost the same. The error margin can be said to be negligible.

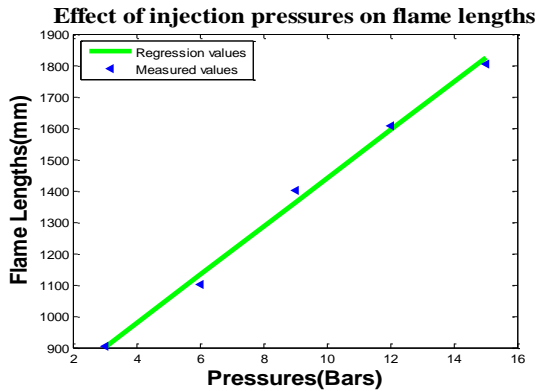


Figure 20: Effect of injected pressures on flame lengths (measured and regression values).

Table 6: Time taken to melt metals [6]

DESCRIPTIONS			
Materials	Quantity (kg)	Time taken to melt material (seconds)	Volume of kerosene used (litres)
Aluminum	0.6	823	0.5
Brass	1.2	1,033	1.0

#### 4. CONCLUSION

The design of the air-blast atomizer was carried out for maximum injection pressure of 15 bars. The experiments of volumetric flow rate, spray lengths, and flame lengths were carried out with the injection pressure ranging from 3 to 15 bars. Experiments showed that at 3 bars, the spray and flame lengths are small and also that at 3 bars; liquid film was not breaking into small droplets. As injection pressure increases from 6 to 12 bars, spray lengths and flame lengths increases due to breaking of liquid film into small droplets. The effect of entrainment of the surrounding air was more at high pressures. The design and construction of this air-blast atomizer like any other atomizer fabricated locally requires little data and is very easy to construct. The atomizer produced the desired result for which it was designed for, in melting the selected metals. It can be concluded that the air-blast atomizer produced can be used for both surface and pit furnaces using kerosene as fuel [6].

#### 5. REFERENCES

- [1] Lefebvre, A. H. 1980. Air-blast Atomization: Prog. Energy science, vol. 6, pp 233 – 261.
- [2] M. J. Madu, I. S. Aji, B. Martins 2014. Design, Construction and Testing of a Burner that uses an admixture of used engine oil and Kerosene for foundry application. International Journal of Innovative Research in Science, Engineering and Technology, vol. 3, issue 9.
- [3] Robert Aftel 1996. Effect of atomization gas properties on droplet atomization in an air-assist atomizer. MSc. Thesis at Virginia Polytechnic Institute and State University, Virginia.
- [4] Lefebvre, A. H., and Ballal, D. R. Gas Turbine Combustion 2010. Alternative Fuels and Emissions, third edition. CRC Press.
- [5] Nigerian National Petroleum Corporation (NNPC) 2007. Warri Refining and Petrochemical Company Ltd, Technical Report, 4:87.
- [6] Benneth Ifenna Okoli 2016. Design and Performance Evaluation of an Air-blast Atomizer, MSc. Thesis, Department of Mechanical Engineering, Lagos State University, Lagos, Nigeria.
- [7] Vasiliov, A.P., Koderaftsov, B.M., Korbatinkov, B.D., Ablintsky, A.M., Polyayov, B.M. Palvian, B.Y. 1993. Principles of Theory and Calculations of Liquid Fuel Jet, Moscow.
- [8] V. A. Borodin, Yu. F. Dityakin, L. A. Klyachko, V. I. Yayodkin 1967. Atomization of liquids, Foreign Technology Division.
- [9] Bayvel, L. 1993. Liquid Atomization. Hemisphere Publishing Corporation, Taylor & Francis.
- [10] Witold Perkowski, Andrzej Irzycki, Krzysztof Snopkiewicz Lukasz Grudzien, and Michal Kawalec 2011. Study on kerosene atomization process under high speed air stream. Journal of Kones Power train and Transport, vol. 18, no 4.
- [11] Pipatpong Watanawanyoo, Sumpun Chaitap and Hiroyuki Hirahara 2009. Development of an air assisted fuel atomizer (liquid siphon type) for a continuous combustor. American Journal of Applied Sciences 6 (3): 380-386.